J Therm Anal Calorim (2011) 103:103–109
DOI 10.1007/s10973-010-1112-2

Experimental investigation of the Nd–Al–Si system

The isothermal section at 500 °C

Anna Maria Cardinale · Daniele Macciò · Stefano Delfino · Adriana Saccone

AICAT2010 Special Chapter

Abstract The isothermal section of the Nd–Al–Si ternary system at 500 °C has been investigated using differential thermal analysis, X-ray diffraction analysis, scanning electron microscopy and electron micro-probe analysis. Four ternary intermetallic compounds were confirmed: $NdAl_2Si_2$ (τ_1), hP5-$CaLa_2O_2$ structure type, Nd_2Al_3Si (τ_2), hP3-AlB_2 structure type, $NdAl_{1-x}Si_{1+x}$, $0.25 \leq x \leq 0.3$ (τ_3), tI12-$\alpha ThSi_2$ structure type and $Nd_2Al_{1-x}Si_{1+x}$, $0 \leq x \leq 0.2$, (τ_5), oS8-CrB structure type. A new ternary intermetallic phase (τ_4) was found: $Nd_4Al_3Si_3$, orthorhombic oS20, isotypic with $Pr_4Al_3Ge_3$.

Keywords Phase diagrams · Intermetallic compounds · Aluminium alloys · Rare-earth alloys · Silicon alloys

Introduction

The development of light weight alloys has received great attention in recent years; in this framework Al–Si-based alloys are widely used in industries for their low thermal expansion, good resistance to wear and other properties that can be improved by the addition of rare-earth elements (R) [1, 2].

Our research group has long been involved in the investigation of R metal alloys with light elements such as Mg and Al. The rare-earth metals constitute a group of elements whose alloying behaviour is interesting not only for the possible technological applications of the R-based alloys but also because these elements represent important additional alloying components to several metals.

In the framework of a general interest in the study of the constitutional properties of light elements with rare-earth metals, an experimental investigation of the Nd–Al–Si isothermal section at 500 °C is the subject of this article.

A. M. Cardinale (✉) · D. Macciò · S. Delfino · A. Saccone
Dipartimento di Chimica e Chimica Industriale, Università di Genova, Via Dodecaneso, 31, 16146 Genoa, Italy
e-mail: cardinal@chimica.unige.it

Literature data

Boundary binary systems

The Nd–Si phase diagram was assessed by Gokhale [3] mainly on the basis of a complete investigation of the phase equilibria carried out by Eremenko et al. [4]. The following intermediate phases have been found to exist: Nd_5Si_3 (tI32-Cr_5B_3 type), Nd_5Si_4 (tP36-Zr_5Si_4 type), NdSi (oP8-FeB type). In the composition range from 55 to 67 at.% Si, three compounds indicated as $NdSi_{2-x}$ have been reported [5]: at $x \sim 0.6$ Nd_3Si_4 (57.14 at.% Si, nearly stoichiometry, oC20-Ho_3Si_4 type), at $x \sim 0.34$ Nd_2Si_3 (60 at.% Si, hP3-AlB_2 type structure, stable at $T < 527$ °C) and in the 64–66.8 at.% Si range the $\sim NdSi_2$ phase, which structure shows an allotropic transformation from tI12-$\alpha ThSi_2$ type to oI12-$\alpha GdSi_2$ type when the temperature decreases from 1753 °C (congruent melting temperature) to the range 7.5–147 °C, depending on the composition.

The Nd–Al phase diagram was recently reassessed by Gao et al. [6] based on previous literature data [7–10] and new additional experimental results. The following intermediate compounds exist: Nd_3Al (hP8-Ni_3Sn type), Nd_2Al (oP12-Co_2Si type), NdAl (oP16-DyAl type), $NdAl_2$ (cF24-$MgCu_2$ type), $\alpha NdAl_3$ (hP8-Ni_3Sn type), $\beta NdAl_3$ (stable at high temperature), αNd_3Al_{11} (oI28-αLa_3Al_{11} type) and βNd_3Al_{11} or $NdAl_4$ (tI10-Al_4Ba type). The Nd-rich region

shows a rather extensive solid solubility of Al in βNd at the eutectic and eutectoid temperatures.

The Al–Si system is a simple eutectic system with the eutectic reaction at 12.2 at.% Si and 577 °C [11].

Nd–Al–Si ternary systems

The partial isothermal section of the ternary system Nd–Al–Si at 500 °C (in the Nd-lean region, less than 50 at.% Nd) has been reported by Long [12]. Two ternary compounds $NdAl_2Si_2$ (hP5-$CaLa_2O_2$ type) and $NdAl_{1+x}Si_{1-x}$ ($0 \leq x \leq 0.4$, tI12-$\alpha ThSi_2$ type) have been confirmed. The ternary compound $NdAl_{1.75}Si_{0.25}$ indicated in the literature [12] as δ can be considered an extension in the ternary field of the binary compound $NdAl_2$, having the $MgCu_2$ type structure. Other Nd–Al–Si intermediate phases have also been studied by other research groups, namely Nd_2Al_3Si (hP3-AlB_2 type) [13] and $Nd_2Al_{1-x}Si_{1+x}$ (oS8-CrB type) [14].

Several papers concerning the phase equilibria and the properties of the systems R–Al–Si (R = rare-earth metal) have been published: La–Al–Si (0–33 at.% La) [15], Ce–Al–Si [16], Pr–Al–Si (0–33 at.% Pr) [13], Nd–Al–Si [12], Sm–Al–Si (partial liquidus projections in the Al-rich part) [17], Eu–Al–Si [18] Gd–Al–Si [19], Al–Si–Ho [20], Al–Si–Er [21] and Al–Si–Y [22].

Table 1 shows the literature data on intermetallic compounds of the R–Al–Si systems.

Experimental procedure

The samples were synthesized by weighing stoichiometric amounts of the constituent elements and then melting them by induction melting or arc-melting (for low content of neodymium), under a stream of pure argon. The metals used as starting materials were supplied by Newmet Koch, Waltham Abbey, England (Al nominal purity 99.999 mass%, Si 99.99 mass%, Nd 99.9 mass%). After melting, the alloys were annealed at 500 °C for 350 h in a resistance furnace and quenched in water.

The alloys have been studied, both in the as cast condition and after annealing, by powder X-ray diffraction (XRD), metallography, scanning electron microscopy (SEM) and electron probe microanalysis (EPMA).

Differential thermal analysis (DTA) was carried out on a number of alloys, both on heating and on cooling, at a rate of 10 K min^{-1}, using samples enclosed in sealed tantalum crucibles. The instrument used was a model 404S Netzsch apparatus (Selb, Germany). Operating conditions and data handling for these techniques are described, for instance, in ref. [9].

Smooth surfaces of specimens for microscopic observation were prepared using SiC papers and diamond pastes down to 1 μm grain size. For the quantitative analysis (SEM/EPMA), an acceleration voltage of 20 kV was applied for 50 s, and a cobalt standard was used for calibration. The software package Inca Energy (Oxford Instruments, Analytical Ltd., Bucks, UK) was employed to

Table 1 Crystal structure data of the intermediate phases of the R–Al–Si systems

Stoichiometry	R, Al/at.%	R	Crystal structure	References
RAl_2Si_2	20, 40	La–Yb, Y	hP5-$CaAl_2O_2$	[13]
$R_3Al_4Si_6$	23.1, 30.8	La, Ce, Pr	hP16-$Ce_3Al_4Si_6$	[14]
$RAlSi_2$	25, 25	Ce, Pr, Nd	hP8-$CeAlSi_2$	[14]
$RAl_{2.8}Si_{0.2}$	25, 50	Er	hP24-PuAl3	[21]
$R_2Al_3Si_2$	28.6, 42.9	Tb, Dy, Ho, Er, Tm, Y	mS14-$Y_2Al_3Si_2$	[23]
$R_5Al_6Si_4$	33.3, 40.0	Er	Unknown	[21]
R_2Al_3Si	33.3, 50	La, Ce, Pr, Nd	hP3-AlB_2	[13]
RAl_xSi_{2-x}	33.3	La, Ce, Pr, Nd, Gd, Tb	tI12-$\alpha ThSi_2$	[24]
		Dy at $T > 700$ °C	tI12-$\alpha ThSi_2$	[25]
		Y, Dy–Tm	oS12-YAlGe	[23]
$R_4Al_3Si_3$	40, 30	Nd	oS20-$Pr_4Al_3Ge_3$	This study
R_2Al_2Si	40, 40	Er	tP10-Mo_2FeB_2	[21]
R_2AlSi_2	40, 20	Ho–Lu, Y	oI10-W_2CoB_2	[26]
$R_2Al_{1-x}Si_{1+x}$	50	La, Ce, Pr, Nd, Sm, Gd	oS8-CrB	[14]
		Er $x = 0.25$	oP8-FeB	
		Er $0.25 < x < 0.5$	cP2-CsCl	
R_6Al_3Si	60, 30	Sm, Gd, Tb, Dy, Ho, Tm, Y	tI80-Tb_6Al_3Si	[27]
		Er	tI80-Tb_6Al_3Si	[21]

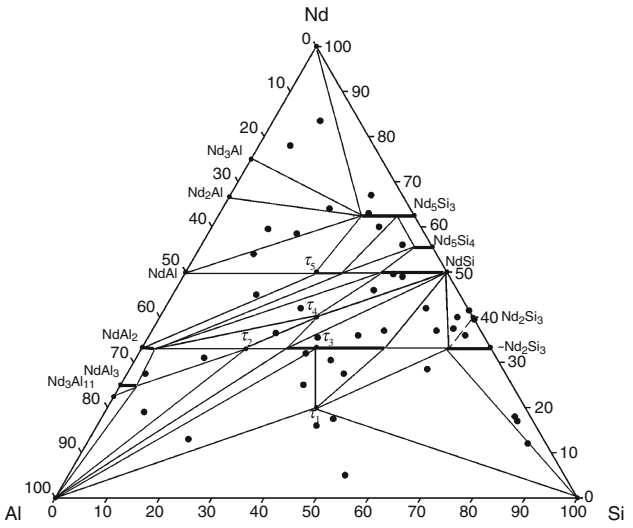

Fig. 1 Nd–Al–Si system. Isothermal section at 500 °C and gross compositions of the analysed Nd–Al–Si alloys (listed in Table 2)

process X-ray spectra. In order to analyse crystal structures and to calculate lattice parameters, X-ray diffraction analysis (XRD) was performed on powder samples using a vertical diffractometer X' Pert MPD (Philips, Almelo, The Netherlands).

Results and discussion

Figure 1 shows the isothermal section of the Nd–Al–Si system at 500 °C, obtained by analysing the annealed alloys of all prepared samples. The dots show the nominal composition of the samples used for the investigation. Results of the SEM/EDX and XRD characterization of selected samples are listed in Table 2. All compositions are given as atomic percent with accuracy ±0.5 at.%.

Selected microphotographs of the analysed alloys are shown in Fig. 2.

Table 2 SEM–EDXS and XRD data on selected Nd–Al–Si samples annealed at 500 °C

Nominal composition/at.%	Phases analysis	Crystal structure	EDXS results Nd, Al, Si/at.%	Lattice parameters/nm		
				a	*b*	*c*
$Nd_5Al_{42}Si_{53}$	τ_1	hP5-$CaAl_2O_2$	20.0, 38.5, 41.5	0.4209(2)		0.6622(3)
	(Si)	cF8-C_{diam}	0.0, 1.5, 98.5			
	(Al)	cF4-Cu	0.0, 99.0, 1.0	0.5093(1)		
$Nd_{12}Al_{3.5}Si_{84.5}$	(Si)	cF8-C_{diam}	1.0, 0.0, 99.0	0.5439(3)		
	$\beta NdAl_xSi_{2-x}$	tI12-$\alpha ThSi_2$	31.5, 11.0, 57.5	0.4186(2)		1.3620(3)
$Nd_{16}Al_{42}Si_{42}$	(Si)	cF8-C_{diam}	0.0, 1.0, 990.0	0.5496(2)		
	τ_1	hP5-$CaAl_2O_2$	22.0, 35.0, 43.0	0.4211(4)		0.6707(5)
$Nd_{13}Al_{68}Si_{19}$	τ_1	hP5-$CaAl_2O_2$	19.5, 40.0, 40.5	0.4199(5)		0.6538(4)
	τ_3	tI12-$\alpha ThSi_2$	31.0, 33.0, 36.0	0.4199(3)		1.4447(3)
	(Al)	cF4-Cu	0.0, 98.5, 1.5	0.4042(2)		
$Nd_{17}Al_3Si_{80}$	(Si)	cF8-C_{diam}	1.5 0.0, 99.5	0.5684(1)		
	$\beta NdAl_xSi_{2-x}$	tI12-$\alpha ThSi_2$	34.0, 6.0, 60.0	0.4125(5)		1.3712(7)
$Nd_{17.5}Al_{38}Si_{44.5}$	(Si)	cF8-C_{diam}	0.0, 0.5, 100.5			
	$\beta NdAl_xSi_{2-x}$	tI12-$\alpha ThSi_2$	33.0, 15.0, 52.0			
	τ_1	hP5-$CaAl_2O_2$	20.0, 37.5, 40.0			
$Nd_{19}Al_{73.5}Si_{7.5}$	$NdAl_{3-x}Si_x$	hP8-Ni_3Sn	26.0, 68.0, 6.0	0.6961(7)		0.5417(5)
	τ_3	tI12-$\alpha ThSi_2$	31.5, 40.5, 28.0	0.4201(6)		1.4513(3)
	(Al)	cF4-Cu	0.0, 99.5, 0.5	0.4044(4)		
$Nd_{18}Al_3Si_{79}$	(Si)	cF8-C_{diam}	1.0, 0.0, 99.0			
	$\beta NdAl_xSi_{2-x}$	tI12-$\alpha ThSi_2$	34.0, 6.0, 60.0			
$Nd_{25}Al_{40}Si_{35}$	τ_1	hP5-$CaLa_2O_2$	20.0, 39.0, 41.0	0.4194(7)		1.4367(4)
	τ_3	tI12-$\alpha ThSi_2$	33.0, 23.5, 43.5	0.4233(7)		0.6694(3)
	(Al)	cF4-Cu (traces)	0.0, 100.0, 0.0			
$Nd_{27.5}Al_{69}Si_{3.5}$	$NdAl_{2-x}Si_x$	cF24-$MgCu_2$	34.5, 63.5, 2.0			
	$NdAl_{3-x}Si_x$	hP8-Ni_3Sn	26.0, 71.0, 3.0			
$Nd_{27.5}Al_{31}Si_{41.5}$	τ_1	hP5-$CaLa_2O_2$	21.0, 38.0, 41.0	0.42128(2)		0.6702(2)
	τ_3	tI12-$\alpha ThSi_2$	34.5, 25.5, 40.0	0.4197(3)		1.4385(4)

Table 2 continued

Nominal composition/at.%	Phases analysis	Crystal structure	EDXS results Nd, Al, Si/at.%	Lattice parameters/nm		
				a	*b*	*c*
$Nd_{28.5}Al_{14.5}Si_{57}$	(Si)	cF8-C_{diam}	0.0, 0.0, 100.0	0.5477(1)		
	$\beta NdAl_xSi_{2-x}$	tI12-$\alpha ThSi_2$	33.5, 13.5, 53.0	0.4183(7)		1.3622(6)
$Nd_{31}Al_{56}Si_{13}$	τ_2	hP3-AlB_2	33.5, 47.5, 19.0	0.4284(3)		0.4211(4)
	$NdAl_2$	cF24-$MgCu_2$	33.0, 64.0, 2.0	0.7986(5)		
	$NdAl_{3-x}Si_x$	hP8-Ni_3Sn	25.5, 70.5, 4.0	0.6444(2)		0.4585(3)
$Nd_{30.5}Al_{32}Si_{37.5}$	τ_3	tI12-$\alpha ThSi_2$	33.5, 25.5, 41.0	0.4195(6)		1.4369(5)
$Nd_{32}Al_{36}Si_{32}$	τ_3	tI12-$\alpha ThSi_2$	32.0, 36.0, 32.0	0.4199(1)		1.4408(2)
$Nd_{35.5}Al_{32}Si_{32.5}$	$NdSi_{1-x}Al_x$	oP8-FeB	47.0, 6.5, 46.5	0.8071(7)	0.3927(5)	0.5896(7)
	τ_1	tI12-$\alpha ThSi_2$	33.0, 38.0, 29.0	0.4217(4)		1.4627(3)
$Nd_{36}Al_{24}Si_{40}$	τ_3	tI12-$\alpha ThSi_2$	34.0, 25.5, 40.5			
	$NdSi_{1-x}Al_x$	oP8-FeB	46.5, 5.5, 48.5			
$Nd_{36}Al_{3.5}Si_{60.5}$	$\beta NdAl_xSi_{2-x}$	tI12-$\alpha ThSi_2$	36.0, 3.5, 60.5	0.4147(4)		1.3707(5)
$Nd_{37.5}Al_5Si_{57.5}$	βdAl_xSi_{2-x}	tI12-$\alpha ThSi_2$	36.0, 4.0, 60.0	4.1568(4)		1.3579(5)
$Nd_{36.5}Al_{39.5}Si_{24}$	τ_4	oS20-$Pr_4Al_3Ge_3$	40.0, 33.0, 27.0	0.4164(8)	2.6144(8)	0.4323(7)
	τ_3	tI12-$\alpha ThSi_2$	34.0, 42.5, 23.5	0.4235(4)		1.4287(5)
	τ_2	hP3-AlB_2		0.4281(3)		0.4235(5)
$Nd_{37}Al_{8.5}Si_{54.5}$	$NdSi_{1-x}Al_x$ $\beta NdAl_xSi_{2-x}$	oP8-FeB	48.5, 1.0, 50.5	0.8169(6)	0.3919(7)	0.5881(7)
		tI12-$\alpha ThSi_2$	35.0, 6.0, 59.0	0.4131(5)		1.3697(4)
	τ_3	tI12-$\alpha ThSi_2$	33.5, 28.5, 38.0	0.4194(3)		1.4454(4)
$Nd_{37}Al_{18.5}Si_{44.5}$	$NdSi_{1-x}Al_x$	oP8-FeB	48.0, 2.5, 49.5	0.8177(6)	0.3924(5)	0.5887(5)
	τ_3	tI12-$\alpha ThSi_2$	34.0, 21.0, 45.0	0.4110(2)		1.4447(3)
$Nd_{40}Al_3Si_{57}$	NdSi	oP8-FeB	48.0, 0.0, 52.0	0.8158(6)	0.3921(7)	0.5881(7)
	$\beta NdAl_xSi_{2-x}$	tI12-$\alpha ThSi_2$	35.0, 4.0, 61.0	0.4155(3)		1.3568(4)
$Nd_{41.5}Si_{58.5}$	$NdSi_{1-x}Al_x$	oP8-FeB	48.0, 0.0, 52.0	0.8166(5)	0.3921(5)	0.5883(6)
	βNd_2Si_3	hP3-AlB_2	36.0, 0.0, 64.0	0.3946(3)		0.4250(3)
$Nd_{42}Al_{32}Si_{26}$	$NdAl_2$	cF24-$MgCu_2$	35.0, 62.5, 2.5	0.7993(1)		
	$NdSi_{1-x}Al_x$	oP8-FeB	48.5, 9.0, 42.5	0.8121(5)	0.3878(7)	0.5875(9)
	τ_4	oS20-$Pr_4Al_3Ge_3$	40.0, 30.0, 30.0	0.4107(6)	2.5987(4)	0.4286(5)
$Nd_{42}Al_8Si_{50}$	$NdSi_{1-x}Al_x$	oP8-FeB	48.5, 0.0, 51.5	0.8175(7)	0.3922(8)	0.5881(8)
	$\beta NdAl_xSi_{2-x}$	tI12-$\alpha ThSi_2$	36.5, 12.0, 51.5	0.4160(4)		1.3591(4)
	$\tau 3$	tI12-$\alpha ThSi_2$	34.0, 24.0, 42.0	0.4193(3)		1.44708(5)
$Nd_{45}Al_{39}Si_{15}$	$NdAl_2$	cF24-$MgCu_2$	34.0, 66.0. 0.0			
	NdAl	oP16-DyAl	50.0, 50.0, 0.0			
	τ_5	oS8-CrB	49.0, 26.0, 25.0			
$Nd_{46}Al_{16}Si_{38}$	$NdSi_{1-x}Al_x$	oP8-FeB	48.0, 6.0, 46.0	0.8153(6)	0.3886(6)	0.5935(8)
	τ_4	oS20-$Pr_4Al_3Ge_3$	39.5, 30.0, 30.5	0.4181(7)	2.5633(5)	0.4293(5)
$Nd_{49}Al_9Si_{42}$	$NdSi_{1-x}Al_x$	oP8-FeB	50.0, 8.0, 43.0	0.8207(6)	0.3944(4)	0.5911(5)
$Nd_{49.5}Al_{10.5}Si_{39.5}$	$Nd_5Si_{4-x}Al_x$	tP36-Zr_5Si_4	54.5, 4.0, 41.5	0.7900(3)		1.4814(2)
	$NdSi_{1-x}Al_x$	oP8-FeB	48.5, 6.0, 45.5	0.8139(5)	0.3931(7)	0.5889(7)
$Nd_{54}Al_{35}Si_{11}$	$Nd_5Si_{3-x}Al_x$	tI32-Cr_5B_3	(traces)	0.7757(7)		1.3813(7)
	NdAl	oP16-DyAl	50.0, 50.0, 0.0	0.5943(6)	1.1744(6)	0.5731(5)
	τ_5	oS8-CrB	50.0, 26.0, 24.0	0.4437(6)	1.1149(6)	0.4067(7)
$Nd_{56}Al_{5.5}Si_{38.5}$	$Nd_5Si_{3-x}Al_x$	tI32-Cr_5B_3	61.0, 4.0, 35.0	0.7730(3)	1.1125(8)	1.3921(4)
	τ_5	oS8-CrB	50.0, 23.0, 27.0	0.4440(7)		0.4095(8)
	$Nd_5Si_{4-x}Al_x$	tP36-Zr_5Si_4	53.5, 3.0, 43.5	0.7882(2)		1.4857(29

Table 2 continued

Nominal composition/at.%	Phases analysis	Crystal structure	EDXS results Nd, Al, Si/at.%	Lattice parameters/nm		
				a	*b*	*c*
$Nd_{59.5}Al_{29.5}Si_{11}$	Nd_2Al	oP12-Co_2Si	67.0, 33.0, 0.0	0.6730(8)	0.5218(8)	0.9652(6)
	$Nd_5Si_{3-x}Al_x$	tI32-Cr_5B_3	61.5, 11.0 25.5	0.7750(3)		1.3723(2)
	NdAl	oP16-DyAl	51.5, 49.5, 0.0	0.5938(7)	1.1760(6)	0.5732(6)
$Nd_{58.5}Al_{24.5}Si_{17}$	Nd_2Al	oP12-Co_2Si	67.0, 33.0, 0.0	0.6719(7)	0.5234(7)	0.9663(8)
	$Nd_5Si_{3-x}Al_x$	tI32-Cr_5B_3	63.5, 10.0, 26.5	0.7768(4)		1.3799(3)
	NdAl	oP16-DyAl	67.0, 33.0, 0.0	0.5936(6)	1.1729(6)	0.5722(7)
$Nd_{60}Al_8Si_{32}$	$Nd_5Si_{3-x}Al_x$	tI32-Cr_5B_3	61.0, 3.0, 36.0	0.7772(2)	1.1133(5)	1.3704(2)
	τ_5	oS8-CrB	51.0, 23.0, 26.0	0.4414(5)		0.4057(6)
$Nd_{63}Al_{8.5}Si_{28.5}$	Nd_3Al	hP8-Ni_3Sn	75.0, 25.0, 0.0	0.6966(3)		0.5406(3)
	$Nd_5Si_{3-x}Al_x$	tI32-Cr_5B_3	61.5, 6.0, 32.5	0.7754(4)		1.3799(2)
$Nd_{64}Al_{15.5}Si_{20.5}$	Nd_3Al	hP8-Ni_3Sn	75.0, 25.0, 0.0	0.6921(4)	0.5202(7)	0.5362(5)
	Nd_2Al	oP12-Co_2Si	67.0, 33.0, 0.0	0.6683(7)		0.9853(5)
	$Nd_5Si_{3-x}Al_x$	tI32-Cr_5B_3	61.0, 6.5, 32.5	0.7758(4)		1.3800(3)
$Nd_{67}Al_6Si_{27}$	αNd	hP4-αLa	99.0, 1.0, 1.0			
	$Nd_5Si_{3-x}Al_x$	tI32-Cr_5B_3	60.5, 3.0, 31.5			
$Nd_{78}Al_{16}Si_7$	αNd	hP4-αLa	92.5, 4.0, 3.5	0.6968(4)		0.5407(4)
	Nd_3Al	hP8-Ni_3Sn	75.0, 25.0, 0.0	0.7720(5)		1.3888(39
	$Nd_5Si_{3-x}Al_x$	tI32-Cr_5B_3	60.0, 12.5, 27.5			
$Nd_{83.5}Al_{7.5}Si_9$	αNd	hP4-αLa	97.0, 1.5, 1.5			
	Nd_3Al	hP8-Ni_3Sn	75.0, 25.0, 0.0	0.6974(5)		0.5390(3)
	$Nd_5Si_{3-x}Al_x$	tI32-Cr_5B_3	61.0, 7.5, 22.5	0.7788(4)		1.3771(6)

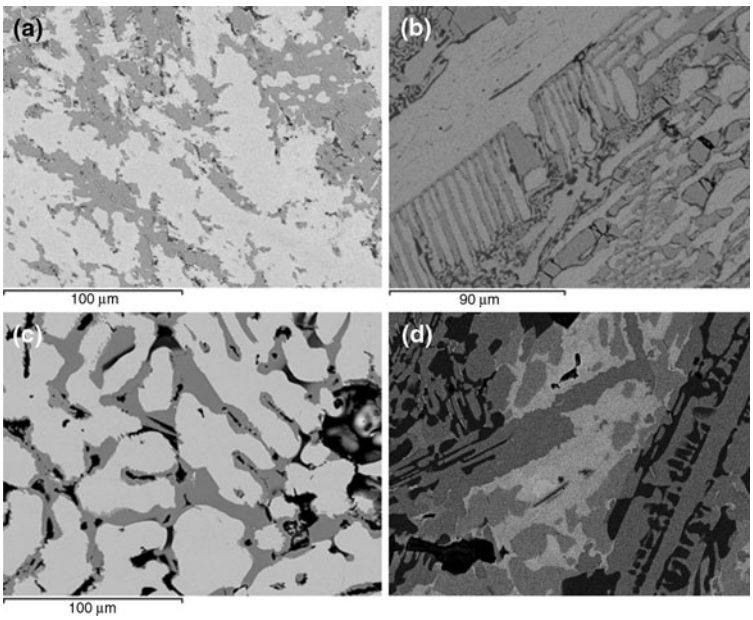

Fig. 2 Back scattered electrons (BSE) images of selected Nd–Al–Si samples, annealed at 500 °C. **a** Sample at 60 at.% Nd, 8 at.% Al: $Nd_5Al_xSi_{3-x}$ (*light grey*) and τ_5 phase (*dark grey*). **b** Sample at 83.5 at.% Nd, 7.5 at.% Al: (Nd) (*white*), $Nd_5Al_xSi_{3-x}$ phase (*light grey*) and very small amounts of Nd_3Al (*black*). **c** Sample at 27.5 at.% Nd, 31 at.% Al: τ_1 (*white*) and τ_3 (*light grey*). **d** Sample at 45 at.% Nd, 39 at.% Al: $NdAl_2$ (*white*), τ_5 phase (*grey*) and NdAl (*black*)

The binary phases $NdAl_3$, $NdAl_2$, ~$NdSi_2$, NdSi, Nd_5Si_4 and Nd_5Si_3 dissolve the third element forming ternary solid solutions: $NdAl_{3-x}Si_x$ $0 \le x \le 0.2$, $NdAl_{2-x}Si_x$ $0 \le x \le 0.06$, $NdAl_xSi_{2-x}$ $0 \le x \le 0.3$, $NdAl_xSi_{1-x}$ $0 \le x \le 0.2$, $Nd_5Al_xSi_{4-x}$ $0 \le x \le 0.3$, $Nd_5Al_xSi_{3-x}$ $0 \le x \le 0.3$. These solid solubility ranges were determined by SEM/EDX quantitative analysis and confirmed by the variation of the lattice parameters. Solid solutions based on binary

Table 3 Lattice parameters of the ternary compounds of the Nd–Al–Si system (this work)

Compound	Crystal structure	Lattice parameters/nm		
		a	*b*	*c*
τ_1 $NdAl_2Si_2$	hP5-$CaLa_2O_2$	0.4212		0.6702
τ_2 Nd_2Al_3Si	hP3-AlB_2	0.4276		0.4204
τ_3 $NdAl_{(1-x)}Si_{(1+x)}$, $x = \sim 0$	tI12-$\alpha ThSi_2$	0.4199		1.4410
τ_4 $Nd_4Al_3Si_3$	oS20-$Pr_4Al_3Ge_3$	0.4107	2.5987	0.4286
τ_5 $Nd_2Al_{(1-x)}Si_{(1+x)}$, $x = 0.25$	oS8-CrB	0.4442	1.1131	0.4043

compounds with the third element amount of less than 1 at.% were not taken into account.

According to the literature data, the two compounds Nd_2Si_3 and Nd_3Si_4 exist in the 55–67 at.% Si. To confirm these compounds, we prepared a few binary Nd–Si samples close to the 2:3 and 3:4 stoichiometric ratios. Only the Nd_2Si_3 was found; samples with compositions close to 57 at.% Si always gave a mixture of NdSi and Nd_2Si_3. DTA performed on a sample corresponding to the $Nd_{41.5}Si_{58.5}$ composition highlighted a thermal effect at 530 °C that is the allotropic transformation of this phase.

A number of ternary phases were found in the Nd–Al–Si isothermal section. Their crystal structure and lattice parameters are reported in Table 3.

The stoichiometric $NdAl_2Si_2$ (τ_1) phase was confirmed to crystallize in the hP5-$CaLa_2O_2$ type structure.

Two phases have been found along the 33.3 at.% Nd: the stoichiometric Nd_2Al_3Si (τ_2) phase and $NdAl_{1-x}Si_{1+x}$ (τ_3) phase existing in a wide homogeneity range ($\sim$25–40 at.% Si). This is in contrast with what was previously reported in the literature for this phase where a homogeneity range from 20 to 50 at.% Si has been suggested [12]. DTA performed on τ_3 samples with a composition corresponding to $x = 0$ (NdAlSi) indicate a melting temperature of 1,440 °C. The micrographic features of the same samples suggest a congruent melting formation for τ_3.

The stoichiometric $Nd_4Al_3Si_3$ (τ_4) phase was not previously reported in the literature. However, phases with the same stoichiometry were found in a number of R–Al–Ge systems (R = La, Ce, Pr, Nd, Sm). The τ_4 phase crystallizes orthorhombic, isostructural with $Pr_4Al_3Ge_3$.

The $Nd_2Al_{1-x}Si_{1+x}$ (τ_5) shows quite a wide homogeneity range at a constant Nd content (50 at.%) from 25 to 30 at.% Si. It was confirmed that it crystallizes in the orthorhombic CrB structure type. The measured lattice parameters agree with those found in literature.

Conclusions

Phase relations of the Nd–Al–Si system were determined at 500 °C in the whole composition range by characterizing about 50 ternary alloys. The three-phase fields and the two-phase fields shown in the isothermal section are 22 and 13, respectively.

The following ternary phases were found to exist:

- The crystal structure of the stoichiometric phases $NdAl_2Si_2$ (τ_1), hP5-$CaLa_2O_2$ and Nd_2Al_3Si (τ_2), hP3 AlB_2 were confirmed.
- The two phases $NdAl_{1-x}Si_{1+x}$ (τ_3), tI12-$\alpha ThSi_2$ and $Nd_2Al_{1-x}Si_{1+x}$ (τ, oS8-CrB type extend, at Nd content constant (33.3 and 50), at 25–40 at.% Si and 20–25 at.% Si, respectively.
- The new ternary phase $Nd_4Al_3Si_3$ (τ_4) is proposed to be isostructural with $Pr_4Al_3Ge_3$, oS20-$Pr_4Al_3Ge_3$ type.

References

1. Miller WS, Zhuang L, Bottema J, Wittebrood AJ, De Smet P, Haszler A, Vieregge A. Recent development in aluminium alloys for the automotive industry. Mater Sci Eng A. 2000;280:37–49.
2. Chen CL, Richter A, Thomson RC. Mechanical properties of intermetallic phases in multi-component Al–Si alloys using nanoindentation. Intermetallics. 2009;17:634–41.
3. Gokhale AB, Munitz A, Abbaschian GJ. The Nd-Si (Neodymium-Silicon) system. Bull Alloy Phase Diagr. 1989;10:246–51.
4. Eremenko VN, Meleshevich KA, Buyanova YuI, Obuskenko IM. The neodymium–silicon system. Dop Akad Nauk Ukr RSR A. 1984;11:77–82.
5. Boulet P, Weitzer F, Hiebl K, Noël H. Structural chemistry, magnetism and electrical properties of binary Nd Silicides. J Alloys Compd. 2001;315:75–81.
6. Gao MC, Ünlü N, Shiflet GJ, Mihalkovic M, Widom M. Reassessment of Al–Ce and Al–Nd binary systems supported by critical experiments and first-principles energy calculations. Metall Mater Trans A. 2005;36A:3269–79.
7. Gschneidner KA Jr, Calderwood FW. The Al–Nd (aluminum–neodymium) system. Bull. Alloy Phase Diagr. 1989;10:28–30.
8. Borzone G, Cardinale AM, Cacciamani G, Ferro R. On the thermochmistry of he Nd–Al alloys. Z Metallkd. 1993;84:635–40.
9. Saccone A, Cardinale AM, Delfino S, Ferro R. Phase equilibria in the rare erath metals (R)-rich regions in the R-Al systems (R = La, Ce, Pr, Nd). Z Metallkd. 1996;87:82–7.
10. Cacciamani G, Ferro R. Thermodynamic modeling of some aluminum-rare earth binary systems: Al–La, Al–Ce and Al–Nd. CALPHAD. 2001;25:583–97.

11. Murray JL, McAlister AJ. The Al–Si (aluminum–silicon) system. Bull Alloy Phase Diagr. 1984;5:74–84.
12. Long Z, Zhou Y, Zhuang Y, Chen R, Liu J, Wang X. Phase relations in the Nd–Al–Si system at 500 °C. J Alloys Compd. 2001;325:190–3.
13. Nakonechna N, Lyaskovska N, Romaniv O, Starodub P, Gladyshevskii E. Pr–Al–Si phase diagram (0–0.33 at.fract. Pr) and crystal structure of the compounds. Visn Lviv Univ Ser Khim. 2001;40:61–7.
14. Lyaskovska N, Romaniv O, Semus'o N, Gladyshevskii E. Crystal structures of the compounds $RAl_{0.5-x}Si_{0.5+x}$ (R = La, Ce, Pr, Nd, Sm, Gd), $R_3Al_4Si_6$ (R = La, Pr), and $RAlSi_2$ (R = Pr, Nd). J Alloys Compd. 2004;367:180–4.
15. Murav'eva AO. The systems La–Al–Si and La–Al–Sb in the region 0–33.3 at% La. Vestn Lviv Univ Ser Khim. 1971;12:8–9.
16. Flandorfer H, Kaczorowski D, Gröbner J, Rogl P, Godart C, Kostikas A. The systems Ce–Al–(Si, Ge): phase equilibria and physical properties. J Solid State Chem. 1998;137:191–205.
17. Markoli B, Spaic S, Zupanic F. The constitution of alloys in the Al-Rich Corner of the Al–Si–Sm ternary system. Z Metallkde. 2001;92:1098–102.
18. Zarechnyuk OS, Yanson TI. The Eu–Al–Si system within a range of 0–33.3 atomic parts of europium. Dopov Akad Nauk Ukr RSR. 1982;4:30–1.
19. Zarechnyuk OS, Yanson TI, Murav'eva AA. The systems Gd–Al–Si, Gd–Al–Ge in the range 0–0.33 of gadolinium. Visn Lviv Univ Ser Khim. 1981;23:64–7.
20. Zhuang YH, Li JQ, Zeng LM. The isothermal section (500 °C) of the phase diagram of the Al–Ho–Si ternary system. J Less-Common Met. 1990;157:47–53.
21. Pukas S, Lasocha W, Gladyshevskii R. Phase equilibria in the Er–Al–Si system at 873 K. CALPHAD. 2009;33:23–6.
22. Murav'eva AO, Zarechnyuk OS, Gladyshevskii EI. The systems Y–Al–Si(Ge, Sb) in the range 0–33.3 at% Y. Izv Akad Nauk SSSR Neorg Mater. 1971;1(7):38.
23. Bobev S, Tobash PH, Fritsch V, Thompson JD, Hundley MF, Sarrao JL, Fisk Z. Ternary rare-earth alumo-silicides—single-crystal growth from Al flux, structural and physical properties. J Solid State Chem. 2005;178:2091–103.
24. Pukas S, Lutsyshyn Y, Manyaco M, Gladyshevskii E. Crystal structures of the RAlSi ans RAlGe compounds. J Alloys Compd. 2004;367:162–6.
25. He W, Zhang JL, Zeng LM. New structure of the ternary compound DyAlSi. J Alloys Compd. 2006;424:105–7.
26. Kranenberg C, Mewis A. Darstellung und Kristallstrukturen von $Ln_2Al_3Si_2$ und Ln_2AlSi_2 (Ln: Y, Tb-Lu). Z Anorg Allg Chem. 2000;626:1448–53.
27. Dubenko IS, Evdokimov AA, Ionov VM. Crystal structure of Tb_6Al_3Si. Sov Phys Crystallogr (Engl Transl). 1987;32:201–3.